Proceedings of 2010 ISFA
2010 International Symposium on Flexible Automation
Tokyo, Japan July 12-14, 2010

UPL-2460

REPETITIVE CONTROL OF A LEVITATED SHAFT - FPGA IMPLEMENTATION BASED ON POWELL-CHAU FILTERS

Herrick Chang
Department of Mechanical and Aerospace Engineering
University of California, Los Angeles
Los Angeles, California 90025
herrick@ucla.edu

Tsu-Chin Tsao*
Department of Mechanical and Aerospace Engineering
University of California, Los Angeles
Los Angeles, California 90025
ttsao@ucla.edu

ABSTRACT

This paper considers high sampling rate digital control of an electromagnetically levitated shaft. Inner loop feedback and outer loop repetitive controls are realized by a Field Programmable Gate Array (FPGA) at 100 kHz rate based on considerations made on limited FPGA computing resources, numerical dynamic range, selection of word length for fixed point computation, and distribution of parallel computing. The benefit of high sampling rate feedback control is demonstrated to reduce the sensitivity peak when compared to lower sampling rate control. The repetitive control involves inverting non-minimum phase zeros and introducing linear phase low-pass filtering for establishing robust stability. These filtering tasks are realized by a modified Powell-Chau filter, which is an efficient infinite impulse response (IIR) realization of high order finite impulse response (FIR) filter. Experimental results are presented to demonstrate the effective control performance.

1 INTRODUCTION

Modern computer numerical control (CNC) machine tools commonly employs digital servo control loops at sampling rate around the order of 2 kHz and achieves about 100 Hz bandwidth for the position feedback loop in each motor driven axis. The advances in digital computing power and their availability in the recent years have made it possible to realize much higher sampling rate digital control for higher precision and servo control performance.

Feedfoward and repetitive control, which are effective in generating precise trajectory generation, involve inversion of system dynamics. However, systems with non-minimum phase zeros cannot be directly inverted. Previous work such as [1], deals with non-minimum phase zeros using zero-phase error tracking controllers (ZPETC). To design a limited bandwidth zero-phase compensation, a high-order finite impulse response (FIR) filter is often required. This poses challenges to high sampling rate realization. An efficient method to realize high order FIR filter is key to performing high sampling rate dynamic inversion in feedforward and repetitive control for precision motion control.

Powell & Chau first introduced the a real-time implementation of a linear phase IIR filter [2]. The realization involves L-length localized time reversals, overlap-add sectioned-convolutions, and another set of time reversals. The end-result produces a linear phase IIR filter with phase equal to that of z^{-4L}. The reset used to truncate the impulse response resulted in parasitic sinusoidal phase disturbances. Thus, resulting in a IIR filter with approximate linear phase. Later, Kurosu [3] proved the imperfections of the Powell-Chau filter analytically and modifies Powell & Chau's structure. Kurosu's modified Powell-Chau filter is proven to have zero phase disturbances. Kurosu exploits the fact that any FIR filter can be represented as the subtraction of two IIR filters. Combining that fact with the Powell-Chau filter, Kurosu introduces a perfectly linear phase IIR filter. The equivalent FIR filter realization would require many more multipliers and adders, up to one or two orders of magnitude, than that of the modified Powell-Chau filter. The authors have previously shown that the Powell-Chau filter can be modified to approximate inversions of non-minimum phase zeros [4]. The realization of the controllers hinge upon implementing a proposed real-time approximate stable inversion of non-minimum phase systems on Field Programmable Gate Arrays (FPGAs), which uniquely suit the application at hand due to parallel computing, speed, and low level interface to physical systems.

In Repetitive Control, zero phase error compensation (ZPETC) [1], which performs stable pole zero cancelation and conjugate compensation on non-minimum phase zeros has been used for approximate inversion in feed-forward and repetitive

*This work was supported in part by the National Science Foundation under Grant CMMI-0751621

controller design. This simple compensator has a form of linear phase stable inversion but has no control over its dynamic range. The inversion structure previously shown by the authors have more flexibility over this dynamic range. This paper discusses the formulation and implementation of a real-time linear phase inversion of non-minimum phase systems through the manipulation of Kurosu's filter implementation.

In addition, Kurosu's exact linear phase filter, can be used to increase the robustness of Repetitive Control. Normally, in order to provide robustness to the discrete-time Repetitive Controller, a linear phase low-pass filter, $Q(z)$, is used as a frequency dependent learning gain [5]. The use of the Kurosu's linear phase IIR filter implementation of linear phase Q-Filter provides a sharp transition band for the magnitude while keeping computational costs low. The paper proposes the Powell-Chau based inversion as part of the Repetitive Control implementation for the levitated shaft system. In addition, the paper demonstrates how Kurosu's Linear Phase IIR filter can assist in the robustness and performance bandwidth of Repetitive Control with very low computational complexity.

The remainder of this paper is structured as follows: Section 2 provides background and motivation for the inversion filter for non-minimum phase zeros. Furthermore, the dynamic range of filter coefficients plays a role when dealing with the inversion of bandlimited systems. Section 3 describes the implementation of Kurosu's filter and provides a basic understanding of linear phase IIR filters. Section 4 shows that the inversion filter is a modified version of Kurosu's filter such that it enables approximate inversions of non-minimum phase zeros. Under certain conditions, the inversion filter with Repetitive Control is appealing due to its computational efficiency. Section 5 discusses the modeling of the levitated shaft along with the effects of discretization when discrete-time controllers are applied. Section 6 places the inversion filter within the Repetitive Control framework. Section 7 provides experimental results performed on a magnetically levitated shaft system which demonstrates the tracking performance of Repetitive Control with a inversion filter. Coupling effects and magnetic nonlinearities are discussed in how it affects performance of different type of controllers.

2 BACKGROUND AND MOTIVATION

In feed-forward controller, inversion compensators are desirable since it controls the plant such that its output follows the reference signal. In addition, the Repetitive Control structure requires the need for some type of feed-forward inversion.

FPGA implementation of controllers typically require fixed-point realization of controllers. As a result, careful consideration for precision and dynamic range of the controllers must taken into account. Through the following sections, it will shown that the Powell-Chau based inversion filter is seemingly more well-behaved in a fixed-point framework. To motivate the implementation of the Q-filter, the computational efficiency between IIR filters and FIR filters are considered.

2.1 Large Dynamic Range

Assuming a physical system with low-pass characteristics, most plant inversions such as H_2, H_∞, ZPETC, etc. tend to compensate by having fairly large high frequency gain. With non-minimum phase zeros, the effect of high frequency gain may be exacerbated by these types of inversions.

Depending on the input signal, the fixed-point filter may require more bits due to the P-norm scaling as addressed in [6]. Scaling and number of 2^{nd}-order cascaded sections used to realize a fixed point filter, affect filter performance as well. Scaling depends on which norm is chosen:

$$||H(i\omega)||_p = \left[\frac{1}{\omega_s}\int_0^{\omega_s} |H(i\omega)|^p d\omega\right]^{\frac{1}{p}} \tag{1}$$

For discrete time and $p = \infty$

$$||H(e^{i\omega})||_\infty = \max_{0<\omega<\omega_s} |H(e^{k\omega})| \tag{2}$$

where ω_s is the sampling frequency in rad/s. For this paper we choose $p = \infty$ to prevent numerical overflow. With finite word-length, the output of the filter can saturate/wrap/overflow. Also the scaling factor may require many bits to represent. This necessity requires an increased of number of bits to represent a larger range while maintaining precision, resulting in more hardware or FPGA gates. The Powell-Chau based inversion filter will lessen these effects.

2.2 Computational Efficiency - FIR vs. IIR

The typical requirement for the Repetitive Control Q-filter is that it be some linear phase low pass filter. It is well known that IIR filters require a much lower order than FIR filters to represent the same magnitude characteristic [7]. However, IIR filters normally does not satisfy linear phase. On the other hand, some FIR filters have linear phase but require order(s) of magnitude more multiplies to realize. By using the Powell-Chau based inversion filter, the linear phase of FIR filters and the computational complexity of IIR filters are now both possible. Regardless of a floating point or a fixed point framework, computational complexity will require more time to compute and/or hardware.

3 LINEAR PHASE IIR FILTER - MODIFIED POWELL-CHAU FILTER

To fully understand the realization of the real-time linear phase IIR filter, we must understand both the real-time FIR case, and the off-line IIR case first. From there, understanding of the Kurosu's modified Powell-Chau Filter will be clear.

3.1 Linear Phase Filters

Traditionally in literature, linear phase filters are FIR filters typically with symmetric taps (coefficients) [7]. In order to make any FIR filter $D(z)$ linear in phase, we can cascade it with $D(z^{-1})$(i.e. $T(z) = D(z) \times D(z^{-1})$).) $D(z^{-1})$ is the complex conjugate of D(z). The resulting $T(z)$ will have linear phase with magnitude response of $|D(z)|^2$ (which was done in [1]). $T(z)$ is noncausal but can be made causal by adding delays. Note that $D(z^{-1})$'s zeros are mirrored images of $D(z)$'s zeros. Thus, stable linear phase filters have mirrored pairs for both their poles and zeros. "Mirrored" in this context is with respect to the unit

circle. For linear phase IIR filters, it would mean their poles would have to come in mirrored pairs. Using traditional filter realizations, linear phase IIR filters are not possible since their conjugates are unstable (i.e. the stable pole's mirror image is an unstable pole). For finite-length sequences such as that in Iterative Learning Control, there are IIR techniques [8] which use time-reversals to cancel out the phase but are not applicable in real-time Repetitive Control.

3.2 Input-Output Relation of Kurosu's Linear Phase IIR filter

Let us first define some notation. Observe the zero-pole-gain form,

$$H(z) = \bar{k}\frac{(z+z_1)(z+z_2)\dots(z+z_r)}{(z+p_1)(z+p_2)\dots(z+p_q)} \tag{3}$$

where, $q \geq r$. This $H(z)$ is the filter choice for within the Powell-Chau filter as seen in Fig. 1. For Kurosu's Filter, $H_{top}(z) = H_{bot}(z) = H(z)$. [3] has proven that Kurosu's filter is linear and time invariant. The exact relation to the modified Powell-Chau filter is:

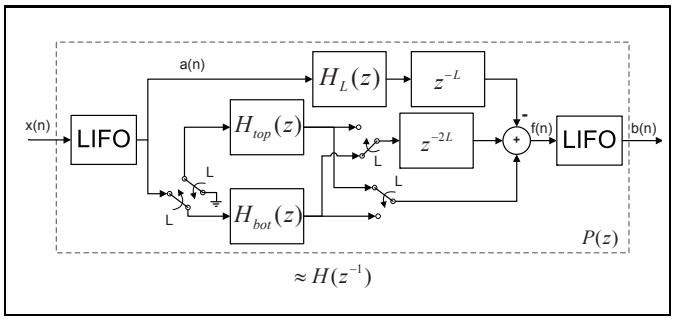

FIGURE 1: Powell-Chau Filter P(z)

Fig. 1 and 2 shows the implementation for the modified Powell-Chau filter and Kurosu's Linear Phase IIR filter, respectively. Exact input-output relation of Kurosu's filter is

$$H_T(z) = H(z) - H_L(z)z^{-L} \tag{4}$$

$$\frac{Y(z)}{X(z)} = H_T(z^{-1})H_T(z)z^{-4L} \tag{5}$$

$$= ||H_T(j\omega)||^2 z^{-4L} \tag{6}$$

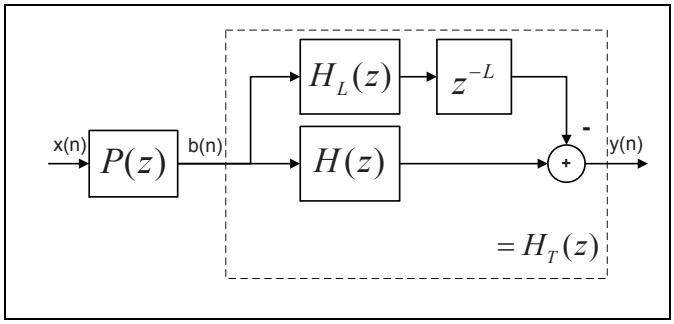

FIGURE 2: Realization of Kurosu's Exact Linear Phase IIR Filter

$H_T(z)$ is an approximation of the impulse response of $H(z)$ up to L samples. $H_L(z)$ is the truncated portion of the impulse response of $H(z)$. Typically, L is chosen where the infinite impulse response (IIR) is near quantization levels. Exact relation $H_L(z)$ is detailed by [3] or estimated by a low order approximation. Also, if L sufficiently long, $H_L(z)$ need not be implemented in fixed-point since coefficient values will be quantized to 0. Thus, $H_T(z)$, $H_T(z^{-1})$ and $H_T(z)\cdot H_T(z^{-1})$ are FIR filters but implemented by IIR filters, switches, and L-word Last-In First-Out (LIFO) memory elements. Operation of the switches and LIFOs are detailed in [2, 3]

As $L \to \infty$, then $H_T(z) \to H(z)$, $H_T(z^{-1})z^{-4L} \to H(z^{-1})z^{-4L}$ and $H_L(z) \to 0$. However, if $H(z^{-1})$ implemented in filter form, it is unstable. This implies that Kurosu's filter has the ability to approximate an unstable filter. We will use this to our advantage in inverting non-minimum phase zeros. Also, note that the modified Powell-Chau filter comes with a delay of 4L. Thus care must be taken when choosing the length of L.

4 INVERSION FILTER

The approximate inverse of non-minimum phase zeros can be performed through a long FIR filter [9]. As seen by [7], long FIR filters are costly in terms of number of multipliers and additions when compared to IIR filters. The proposed inversion is comparable in delay to a FIR filter inversion filter, if not more. However, the main advantage is that the number of multipliers/adders can be reduced by an order of magnitude since it is implemented with IIR filters. From an implementation stand point in both floating-point and fixed-point, the reduction of multiplications/additions enable shorter sampling periods or higher sampling rates. It also frees up more resources to add more compensators if dealing with a MIMO system. *The conditions for the inversion to work properly is that the plant is stable and that zeros are not on the unit circle*. The feed-forward structure can be seen in Fig. 3. Different choices of P and C are detailed below and in Table 1. We denote F to be the feedforward controller F(z), i.e. ($F(z) = P(z)C(z)$).

Define R-conjugate filter as,

$$H^R(z) = \underbrace{\left(\bar{k}\frac{z_1 z_2 \dots z_r}{p_1 p_2 \dots p_q}\right)}_{\gamma} \frac{(z+\frac{1}{z_1})(z+\frac{1}{z_2})\dots(z+\frac{1}{z_r})}{(z+\frac{1}{p_1})(z+\frac{1}{p_2})\dots(z+\frac{1}{p_q})} \tag{7}$$

γ is used to characterize the gain of the conjugate filter. Note that when relative order of $H(z)$ is not 0, then H^R and $H(z^{-1})$ from Section 2 are not the same. R-conjugate is applicable when observing the choice of $H_{top}(z)$ and $H_{bot}(z)$ for the inversion filter shown below.

4.1 Choice of $H_{top}(z)$ and $H_{bot}(z)$

For any given plant,

$$G(z) = k\frac{B^+(z)B^-(z)}{A(z)} \tag{8}$$

where $A(z)$, $B^+(z)$, and $B^-(z)$ are the stable poles, stable zeroes, and unstable zeros, respectively. Let the proposed inversion

Controller	H(z) =	C(z) =	Y(z)/R(z)
Approx. Inv.	$\frac{\gamma M_2}{B^{-R}(z)}$	$\frac{A(z)M_1}{kB^+(z)}$	$\approx z^{-4L-D+D_H}$
IIR-ZPETC	$G(z)$	1	$\approx \|\|G(z)\|\|^2 z^{-4L}$
ZPETC	$\frac{B^-(z)}{kB^-(1)^2}$	$\frac{A(z)}{B^+(z)}$	$= \frac{\|\|B^-(z)\|\|^2}{B^-(1)^2} z^{-4L-D+D_H}$

TABLE 1: Choices of $H(z)$ inside $P(z)$ filter and $C(z)$

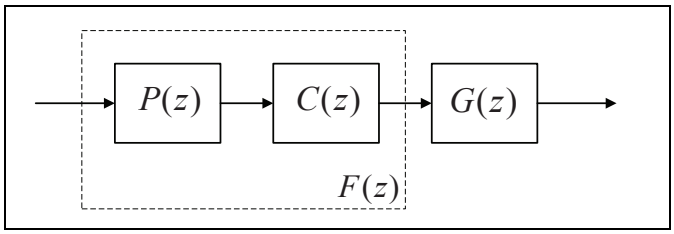

FIGURE 3: Realization of Approximate Non-minimum phase-zero Inversion

controller be $F(z) = P(z)C(z)$. Depending on the choice of $C(z)$, $Y(z)/R(z)$ will be different as seen in Table 1. The $H_{top}(z)$ and $H_{bot}(z)$ in P(z) of Figure 1 can be altered to produce different compensators.

4.1.1 Inversion Filter $C(z)$ is the inversion of stable poles/zeros, assuming a stable plant $G(z)$.

$$C(z) = \frac{A(z)}{kB^+(z)z^{-D}} M_1 \tag{9}$$

$$D = deg(A) - deg(B^+) \tag{10}$$

$$D_H = \text{relative order}(H_{top}) \tag{11}$$

where $deg(\cdot)$ stands for order (or number of roots). By letting $H_{top}(z)$ and $H_{bot}(z)$ inside $P(z)$ be equal to $\frac{\gamma}{B^{-R}(z)} M_2$, approximate inversions of non-minimum phase zeros is possible. Since most physical systems would be bandlimited, M_1 can be chosen to be the reference model. Similary, M_2 can be designed such that the reference model is linear in phase. For simplicity, we will assume $M_1 = M_2 = 1$. Ideally, a stable inversion is desired such that

$$P(z) = H_T(z^{-1})z^{-4L} \tag{12}$$

$$\approx \frac{1}{k} \cdot \frac{1}{B^-(z)} z^{-4L} \tag{13}$$

Recall from the previous section, $P(z)$ can not be realized in any standard filter form since it is unstable. However, using the modified Powell-Chau Filter as seen in Fig. 3, we can obtain a approximate inverse. Letting $H(z)$ be the inverse of the mirrored unstable zero as illustrated in Fig. 3 will produce an approximate inversion. Then, $C(z)$ will invert all stable poles/zeros.

Using Equation 4 and 6, the above choice of $H(z)$

$$H_T(z) = \frac{\gamma}{B^{-R}(z)} - \left[\frac{\gamma}{B^{-R}(z)}\right]_L \cdot z^{-L} \tag{14}$$

satisfies Eqns. 12 and 13

4.1.2 IIR-ZPETC If $H_{top}(z) = H_{bot}(z) = G(z)$ and $C(z) = 1$, this would result in Kurosu's filter with $P(z)$ in cascade with the physical plant. Since this $G(z)$ is not a FIR filter, $P(z) \approx G(z^{-1})z^{-4L}$. We will denote this choice of $H(z)$ and $C(z)$ as the IIR-ZPETC as $Y(z)/R(z)$ is linear-phase (i.e. $Y(z)/R(z) = ||G(i\omega)||^2 z^{-4L}$). However, the major drawback of this method is that if $G(z)$ were to have low-pass characteristics, as most physical system do, the bandwidth would be more limited that that of the above inversion filter.

4.1.3 ZPETC It is interesting to note that if $H_{top}(z) = H_{bot}(z) = \frac{B^-(z)}{kB^-(1)^2}$ and $C(z) = \frac{A(z)}{B^+(z)}$, we will obtain a delayed version of ZPETC [1]. Since $B^-(z)$ is a FIR filter, then if L chosen to be the order of $B^-(z)$ then $P(z) = B^-(z^{-1})z^{-4L}$. Practically speaking, it would be better to implement the standard ZPETC. Assuming that ZPETC can be considered a special case of the Powell-Chau filter, it implies that wherever ZPETC is used, that IIR-ZPETC and the inversion filter may be possible alternatives.

Comparing the Proposed Inversion Filter $F(z)$ with ZPETC and IIR-ZPETC, we find that $F(z)$ will result in tracking a delayed reference, but in exchange does not have the bandwidth issue that ZPETC and IIR-ZPETC has. If a bandlimited system is required, that is where M_1 and M_2 are used to design the reference model.

5 LEVITATED SHAFT

Experiments were performed on a Magnetic Moments MBC 500 levitated shaft system. Although a Multi-Input Multi-Output System (MIMO), through system identification and dynamic decoupling/transformations, the 4-input 4-output system is decoupled into 4 separate Single-Input Single-Output (SISO) systems. For simplicity and brevity, we observe only the Y-axis translational and rotational systems.

5.1 Modeling of Levitated Shaft

After a system identification and a dynamic decoupling of the y-axis translational and rotational system, the transfer functions are:

$$G_{tran}(s) = \frac{-681.1214(s-1651)(s+1381)}{(s+4045)(s+417.3)(s-387.3)} \tag{15}$$

$$G_{rot}(s) = \frac{-589.6263(s-2582)(s+1612)}{(s+4070)(s+428)(s-441.6)} \tag{16}$$

As with most electromagnetic systems, our plants exhibit unstable poles. Furthermore, both rotational and translational plants exhibit similar pole/zero locations. Another important characteristic of the models are that both exhibit non-minimum phase zeros. When implementing repetitive control on the stabilized system, the non-minimum phase zeros play an important role. Detailed modeling and decoupling of this system can be seen in [10]. It shows that the Y-axis and X-axis have very little effect one another which justifies our analysis of only the Y-axis. However, it also shows that the decoupling of the Y-axis into Translational and Rotational are good up to a certain point and still exhibit some minor yet significant coupling effects.

5.2 Stabilizing Controller

Eqn. 15 shows that the decoupled systems are unstable. Thus, a simple lead controller with negative feedback is necessary to stabilize the closed-loop system. The controller was designed to reduce low frequency sensitivity. Since, both the rotational and translational plants are similar, the stabilizing lead controller can be used for both axes. The controller designed is:

$$K(s) = \frac{3.0281(s+430.7)}{(s+1628)} \tag{17}$$

5.3 Effects of Discretization on Sensitivity Function

The continuous-time sensitivity function is:

$$\mathbf{S} = \frac{1}{1+KG} \tag{18}$$

$$= \frac{(s-387.3)(s+417.3)(s+1628)(s+4045)}{(s^2+1080s+3.005\times10^5)(s^2+2561s+3.198\times10^6)} \tag{19}$$

In order to implement advanced discrete time controllers, the plant and lead controller must be discretized. The plant and lead controller will be discretized using a Zero-Order Hold transformation and Tustin (Trapezoidal) Transformation, respectively. Figure 4 illustrates how the different sampling time differs from the continuous-time sensitivity function [11]. This gives an idea of which sampling frequency would be sufficient.

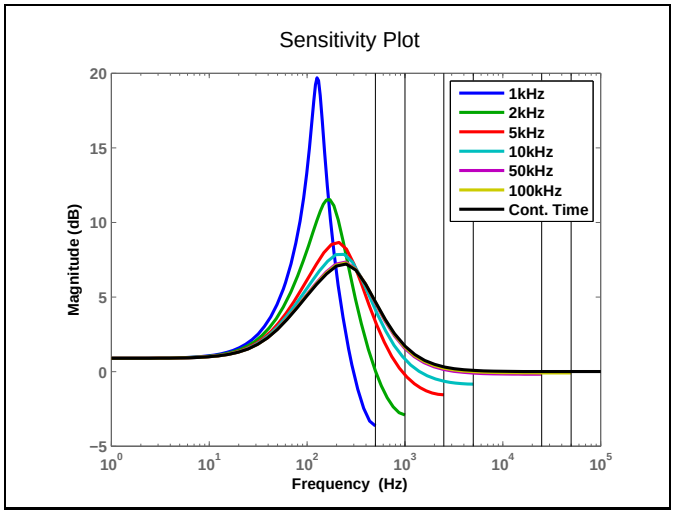

FIGURE 4: Sensitivity Function with different Sampling Rates

As expected, the sensitivity function with higher sampling rates will be resemble the continuous time version. Choosing 100kHz for the sampling rate for the lead controller will make the stabilized closed loop approximate its continuous-time counterpart. The resulting discrete controller and plants are:

$$K(z) = \frac{3.0281(z-0.9957)}{(z-0.9839)} \tag{20}$$

$$G_t(z) = \frac{-0.047872(z-0.9916)(z-0.9863)(z-1.017)}{(z^2-1.992z+0.9924)(z^2-1.97z+0.9712)} \tag{21}$$

$$G_r(z) = \frac{-0.041298(z-0.9916)(z-0.984)(z-1.026)}{(z^2-1.988z+0.9884)(z^2-1.968z+0.9689)} \tag{22}$$

$G_t(z)$ and $G_r(z)$ represents the discretized translational plant and rotational plant, respectively. From here we will assume that translational plant and rotational plant are completely decoupled. For brevity, we will address only the translational plant since control design and issues will the rotational plant will be similar. Although 100kHz is not necessary for the levitated shaft system, it is interesting to observe the inversion filters fixed point behavior at higher sampling rates. If the fixed-point properties are well-behaved, then it may show that the inversion filter can work for systems with a higher bandwidth.

6 REPETITIVE CONTROL OF LEVITATED SHAFT

Repetitive Control (RC) is useful in learning periodic reference. One case of Repetitive Control is the Zero-Phase Error Tracking Control (ZPETC) implementation. In a high-sampling rate and fixed-point framework, ZPETC will have issues with non-minimum phase zeros when used in the structure from Fig. 5. As such, the proposed inversion technique will be useful in replacing ZPETC for this case (in terms of implementation).

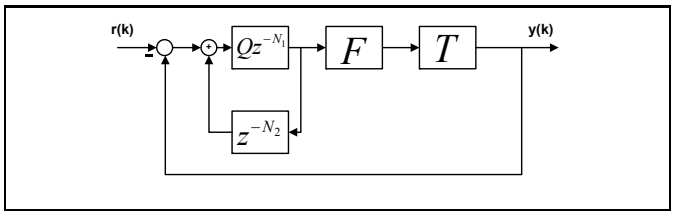

FIGURE 5: Repetitive Control with Feedforward Inversion and Lead controller

6.1 Repetitive Control with ZPETC

First, the traditional ZPETC [1] was attempted and obtained the following filter:

$$F_{zp}(z) = \left[\frac{1}{kB^-(0)^2}\right]\frac{B^-(z^{-1})A(z)}{z^2B^+(z)} \tag{23}$$

$$= 1.83\times10^5\frac{(z-0.9836)A(z)}{z^3B^+(z)} \tag{24}$$

The ZPETC F_{zp} has issues with its dynamic coefficient range as mentioned in Section 2. In order to satisfy the dynamic range and provide enough precision, 16-bit computation will not be enough. Higher-bit computation would be required to represent the range and precision.

Looking at Fig. 6, the ZPETC shows a larger dynamic range as mentioned in 2. Note that we ignore the phase as both compensators are linear phase. Observe $F_{ZP}(z)$ is at -60dB at the low frequencies range and 110dB at high frequencies. Such amplification at high frequencies would cause high-frequency noise or even quantization noise to be greatly amplified or possible fixed-point numerical overflow/saturation. It is worth mentioning that the ZPETC can be cascaded with a linear-phase low-pass filter to lower the large gain at high frequency but would require additional computational complexity. Even if a learning gain were to lower the amplification of high-frequencies, it would push lower frequencies to 16-bit quantization levels. Note that the dynamic range is around 170dB. This ends up being around 29 bits just to represent the filter. Additional bits will be needed for the representation of the input signal. Thus, forcing the implementation to be easily 32-bits or higher.

For this case, our ZPETC was unable to be implemented on the FPGA since estimated computation time was longer than the sampling interval along with not having a sufficient amount of multipliers to carry out the controller. This is one example to demonstrate the computational efficiency between ZPETC and the proposed filter at high-sampling rates. An alternative is to reduce the sampling rate in order to lower the high frequency gain. However, a linear phase filter will still need to be cascaded to ZPETC to reduce the high frequency gain and approximate the inversion of the non-minimum phase zeros. Thereby, increasing computational complexity.

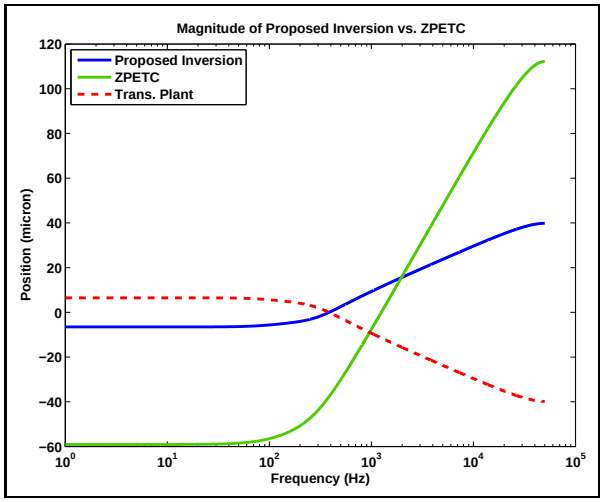

FIGURE 6: Magnitude Comparison of ZPETC and Inversion Filter

6.2 Repetitive Control with Approximate Inversion

A feed-forward controller using the inversion filter was created to help track a delayed reference by inverting the closed-loop stable plant T. T is stabilized with the lead controller from Eqn. 20. Then it is placed into the Repetitive Control structure as seen in Fig. 5. $P_1(z)$, $P_2(z)$, $C_1(z)$ and $C_2(z)$ were chosen to minimize L and adjust the dynamic range and coefficient range to fit within a 16-bit framework. The subscript 1 and 2 denote the translational and rotational model, respectively. The main drawback of the proposed inversion is the $4L$ delay. Fortunately, the delay can be absorbed into the Repetitive Controller. For the levitated shaft system, L_1=L_2=500 for both F_1 and F_2.

$$P_1(z) = \frac{6.9641(z^2 - 2.011z + 1.011)}{z(z - 0.9836)} \tag{25}$$

$$P_2(z) = \frac{7.4348(z^2 - 2.018z + 1.019)}{z(z - 0.9745)} \tag{26}$$

$$C_1(z) = \frac{6.9641(z^2 - 1.975z + 0.9751)}{(z - 0.9957)(z - 0.9863)} \tag{27}$$

$$C_2(z) = \frac{7.4348(z - 0.9957)(z - 0.9843)}{(z - 0.9957)(z - 0.984)} \tag{28}$$

The repetitive control was designed for a fundamental frequency at 25Hz and $f_s = 100kHz$ with $N_1 = N_2 = 2000$. This is designed such that tracking reference signals of 25Hz and its harmonics is possible.

6.3 Repetitive Control Q-Filter using Kurosu's Filter

To ensure robustness of the Repetitive Controller, a linear phase low-pass filter is often chosen. Recall that Section 2.2, motivated the discussion between FIR and IIR filters. A sharp gain drop-off enables the closed-loop system to achieve robustness without sacrificing the closed loop bandwidth. Kurosu's linear-phase IIR filter, as seen in Figure 2, is the compromise between the two. It uses the computational complexity of an IIR filter while retaining the linear phase of an FIR filter. This implementation is ideal for the low-pass Q filter in repetitive control.

To realize the robustness Q filter, we can simply design any IIR filter $Q_{base}(z)$ with any standard filter design techniques [7] to obtain the desired magnitude characteristic. After placing this filter in the Kurosu's Filter from Section 3 , the resulting filter will become $||Q_{base}||^2 \cdot z^{-4L_q}$. There are also many other linear phase IIR variations using the Powell-Chau filter such as [12]. From [5], a sufficient condition for the Repetitive Controller to be robustly stable is by designing a Q such that it is lower than inverse of the multiplicative modeling error, i.e. $Q < \frac{G}{|G-\hat{G}|}$. G is the actual plant data and $\hat{G}$ is the plant model.

For the levitated shaft, it also serves another purpose. Due to coupling effects, there is a 2.5kHz disturbance in which the Repetitive Control cannot compensate. More specifically, if 2.5kHz disturbance were to affect the plant, its phase is perfectly 180° such that the Repetitive Control will become unstable. This coupling effect is due to model inaccuracies. The inaccuracies originate from the dynamic decoupling of the translational and rotational systems as mentioned in [10]. Consequently, our Q filter must eliminate the frequency 2.5kHz. An IIR filter with

corner frequency 500Hz to eliminate the 2.5kHz coupling disturbance satisfying robustness as shown in Fig. 7.

$$Q_{base}(z) = \frac{0.00041651(z+1)^2}{(z^2 - 1.941z + 0.9431)} \quad (29)$$

$$Q(z) = ||Q_{base}(z)||^2 \cdot z^{-200} \quad (30)$$

Observe that the Q-filter is an 2^{nd} order IIR filter. As a comparison, an equivalent FIR filter designed in MATLAB, satisfying the same corner frequency gain drop-off, is a $43^{th} FIR filter$. Thus, showing an order of magnitude of savings for the Q-filter. The designed IIR filter is then placed in Kurosu's Linear Phase IIR filter structure to obtain exact linear phase. Approximate impulse response length was chosen to be $L_q = 400$. Thus, N_q=800.

Based on the ZPETC-style Repetitive Control from Figure 5, we can obtain some sensitivity analysis. For lead control with Feedforward and Repetitive Control and assuming F is a nearly perfect inversion:

$$S_{Lead+RC} \approx \frac{(1-Qz^{-N})}{(1-Qz^{-N}+z^{-N+4L+Nq})} \quad (31)$$

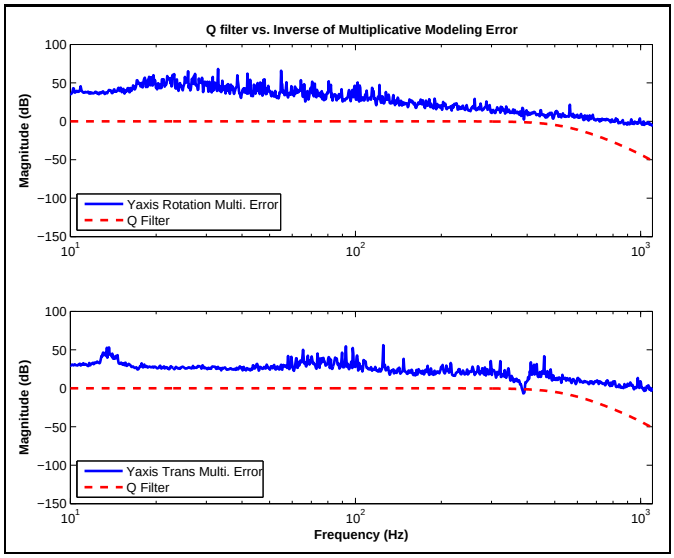

FIGURE 7: Magnitude of Q filter vs. Inverse of Multiplicative Modeling Error for Robust Stability of Translational and Rotational Systems

7 EXPERIMENTAL RESULTS

The controller was implemented on a Labview PXI-7833R FPGA board. Experiments were conducted while applying an external 1.22V triangular wave reference signal of 50Hz to the translational system. The output motion, measured by a Hall effect sensors, of levitated shaft translates to approximately $100\mu m/V$. Thus, the translational reference is a $122\mu m$ triangular profile. Rotational input is regulation (i.e. reference is 0V). Assuming small angles, the conversion is $1.3699 mrad/V$.

From Fig. 8, the error from the lead controller shows that there is coupling present between rotational and translational axes. Coupling can be seen from the periodic reference showing up in the output of the rotational model. Recall, that Repetitive Controller tracks periodic references as well as reject periodic disturbances as seen in Fig. 9. For the levitated shaft, repetitive controllers were designed for both translational and rotational systems to reject the periodic disturbances generated from coupling effects.

The total travel for the shaft is approximately $\pm 300\mu m$ in the translational directions. The models used in this paper are linearized around an equilibrium point. Looking at Fig. 8, the lead controller produces a "parabolic" shape at the translational output is due to magnetic nonlinearity. Fortunately, it appears that the repetitive control helps compensate for this nonlinearity.

The RMS error values for the lead and Repetitive Control are listed in Table 2. Since the rotational movement is under regulation with Repetitive Control, the error value is indicative of the noise level. In this context, "noise" refers to both electrical noise from the sensor and the quantization/round-off "noise" introduced by fixed point arithmetic/multiplications. The increase in quantization noise is explained by the increased number of fixed-point calculations(i.e. more complex controllers). Depending on the filter structure used, quantization noise can be reduced [7]. For this application, Direct Form II Cascaded Transposed Second Order Sections provided the best compromise between quantization, number of bits, and number of adders/multipliers.

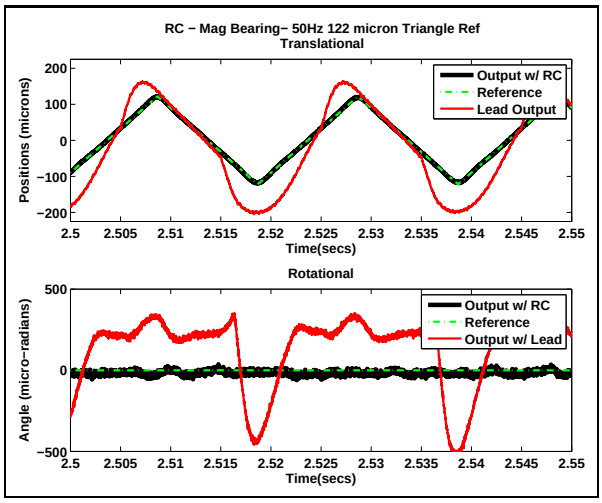

FIGURE 8: Tracking Performance Comparison of Lead and Proposed Repetitive Controller

From Table 2, it is obvious when tracking periodic signals that Repetitive Controllers have much lower errors. Note, that ZPETC Repetitive Control is not compared here because it requires more hardware than the current setup is capable of.

8 CONCLUSION

The experimental results have demonstrated the benefit of high sampling rate digital feedback control in reducing the sen-

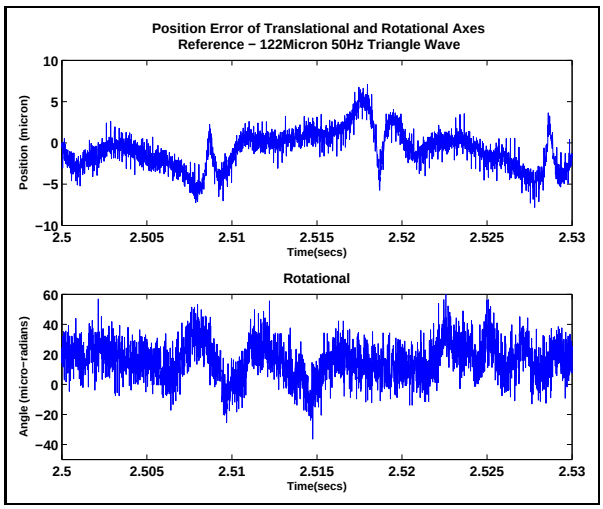

(a) Time Domain

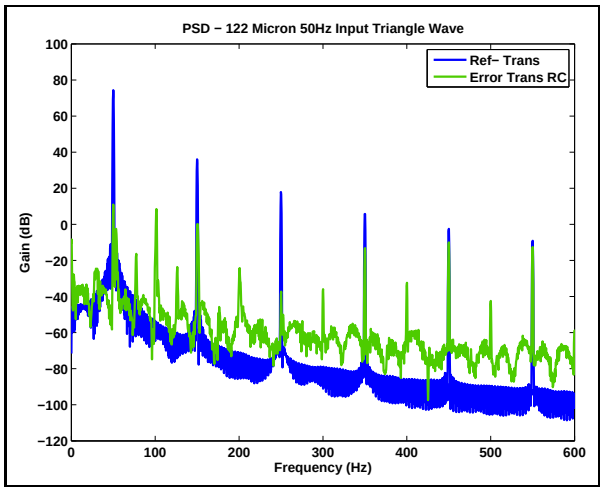

(b) Power Spectral Density

FIGURE 9: Position Error of Proposed Repetitive Controller

Controller	Translation Error	Rotation Error
Lead	123.42μm rms	258.2599 μrad rms
RC	12.65 μm rms	43.1141 μrad rms

TABLE 2: Error RMS values, Translation Reference 122 micron Triangle Wave and with Rotational Regulation

sitivity peak. For trajectory tracking, the modified Powell-Chau filter has been shown to be an efficient way to realize high order FIR filters in the zero-phase inversion filters as well as zero-phase low-pass filters. The Powell-Chau filter reduces multiplications/additions in exchange for a longer delay. The computational efficiency allows multiple compensators to be implemented on the FPGA for the MIMO levitated shaft. The inversion filter employed by the Repetitive Controller provides for precise tracking of periodic signals. To maintain the computational efficiency, robustness, and performance, Kurosu's linear phase IIR filter realization of the Q filter was introduced. By replacing the linear phase FIR Q-filter with Kurosu's IIR filter, an order of magnitude of multipliers has been saved. The experimental results have demonstrated the effectiveness of these proposed approaches in generating precise trajectories.

REFERENCES

[1] M. Tomizuka, "Zero phase error tracking algorithm for digital control," *Journal of Dynamic Systems, Measurement, and Control*, vol. 109, no. 1, pp. 65–68, 1987. [Online]. Available: http://link.aip.org/link/?JDS/109/65/1

[2] S. Powell and P. Chau, "A technique for realizing linear phase iir filters," *Signal Processing, IEEE Transactions on*, vol. 39, no. 11, pp. 2425–2435, Nov 1991.

[3] A. Kurosu, S. Miyase, S. Tomiyama, and T. Takebe, "A technique to truncate iir filter impulse response and its application to real-time implementation of linear-phase iir filters," *Signal Processing, IEEE Transactions on*, vol. 51, no. 5, pp. 1284–1292, May 2003.

[4] H. Chang and T.-C. Tsao, "Efficient fixed-point realization of approximate dynamic inversion compensators for non-minimum phase systems," in *American Control Conference, 2010. Proceedings of the 2010*, will appear June 2010.

[5] T.-C. Tsao and M. Tomizuka, "Robust adaptive and repetitive digital tracking control and application to a hydraulic servo for noncircular machining," *Journal of Dynamic Systems, Measurement, and Control*, vol. 116, no. 1, pp. 24–32, 1994. [Online]. Available: http://link.aip.org/link/?JDS/116/24/1

[6] L. Jackson, "Roundoff-noise analysis for fixed-point digital filters realized in cascade or parallel form," *Audio and Electroacoustics, IEEE Transactions on*, vol. 18, no. 2, pp. 107–122, Jun 1970.

[7] S. K. Mitra, *Digital Signal Processing: A Computer-Based Approach*. McGraw-Hill, 2004.

[8] J. Ghosh and B. Paden, "Iterative learning control for nonlinear nonminimum phase plants," *Journal of Dynamic Systems, Measurement, and Control*, vol. 123, no. 1, pp. 21–30, 2001. [Online]. Available: http://link.aip.org/link/?JDS/123/21/1

[9] E. Widrow, B. Walach, *A Signal Processing Approach*. John Wiley & Sons, 2008.

[10] K. Chu, Y. Wang, J. Wilson, C.-Y. Lin, and T.-C. Tsao, "Modelling and control of a magnetic bearing system," in *American Control Conference, 2010. Proceedings of the 2010*, will appear June 2010.

[11] H.-K. Sung and S. Hara, "Properties of sensitivity and complementary sensitivity functions in single-input single-output digital control systems," *International Journal of Control*, vol. 48, no. 6, pp. 2429–2439, 1988.

[12] J. Willson, A.N. and H. Orchard, "An improvement to the powell and chau linear phase iir filters," *Signal Processing, IEEE Transactions on*, vol. 42, no. 10, pp. 2842–2848, Oct 1994.